SUPPORTING INFORMATION

Spatial resolution of coherent cathodoluminescence super-resolution microscopy

Joris Schefold,[1] Sophie Meuret,[1] Nick Schilder,[1] Toon Coenen,[1,2] Harshal Agrawal,[1] Erik C. Garnett,[1] and Albert Polman[1]*

[1]Center for Nanophotonics, AMOLF, Science Park 104, 1098 XG Amsterdam, the Netherlands

[2]Delmic B.V., Kanaalweg 4, 2628 EB, Delft, The Netherlands

(5 pages and 2 figures)

1) Electron excitation energy spectrum

Figure S1 shows the time evolution of the radial and axial electric field intensity at a fixed position 5 nm away from a trajectory of a 30 keV electron. The field components form a single oscillation in a period of several 100 attoseconds. The corresponding energy spectrum spans a broad range from 0 to ~40 eV: the spectrum monotonously decreases with energy for the radial component while for radial component it peaks at ~8 eV. This broad spectrum makes high-energy electrons an effective broadband source of excitation in the optical spectral range. The plasmon resonances in the 2.2-3.2 eV spectral range (see Figure 1a) can be readily excited by the 30 keV electron.

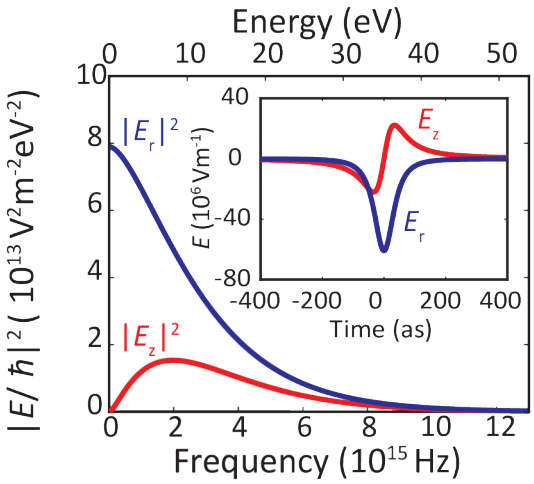

Figure S1. Inset: Time evolution of the radial (E_r) and axial (E_z) electric field intensity 5 nm away from the trajectory of a 30 keV electron in vacuum. Main panel: Fourier transform showing the corresponding energy spectra.

2) SEM/CL experiments

CL experiments were performed using a Thermo Fisher/FEI Quanta 650 FEG SEM equipped with a Delmic SPARC CL collection and analysis system equipped with a photomultiplier tube in combination with a bandpass filter, and Czerny-Turner spectrometer equipped with a CCD array detector. The typical beam current in the CL measurements was 0.5-5nA. CL spectra were normalized using measurements and calculations of transition radiation on an Al surface.[1] For all spectral measurements we collect a substrate reference and subtract it from the data. CL line scans were taken using a Hamamatsu H10721-20 photomultiplier tube, sensitive in the 1.3-5.4 eV spectral range using 1 nm steps. Coarse spectral CL maps were taken with a 11 nm pixel size. Figure S2 shows maps of the dipolar and corner modes at 2.5 eV and 3.1 eV, respectively. Secondary electrons were collected with an Everhart-Thornley detector that is aligned with optical axis of the paraboloid mirror and faces the open end of the mirror. The HAADF-STEM image in Figure 1b is taken using a Thermo Fisher/FEI Verios G4 XHR SEM.

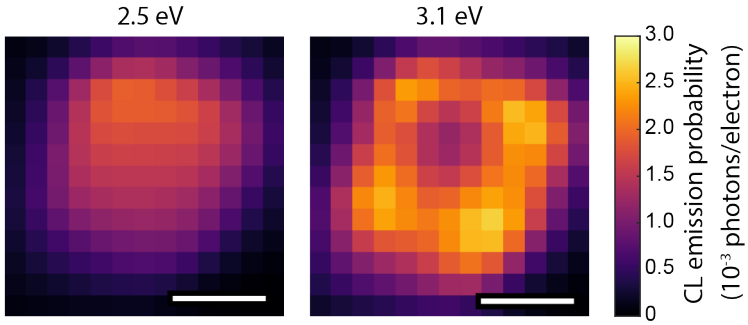

Figure S2. Spatial CL maps (30 keV) of a 70 nm Ag nanocube at 2.5 eV and 3.1 eV, using a collection bandwidth of 40 nm. Scale bar = 50 nm.

3) Ag nanocube synthesis

Single-crystalline Ag nanocubes were made using chemical synthesis originally described in Ref. 2 and drop-cast onto a 15-nm-thick low-stress Si_3N_4 membrane (Silchem) to create a near-symmetric dielectric environment for the nanocubes and avoid unwanted incoherent CL from the substrate. The particle sizes are in the range 75 ± 5 nm. Prior to the CL measurements polyvinylpyrrolidone ligands were removed from the Ag nanocubes using sodium borohydride to minimize the build-up of carbon contamination during electron irradiation.

4) CASINO simulations

Simulations were done for a 70 nm Ag cube without substrate. A total of 10^5 primary electron trajectories was simulated for each incident beam position for 10 keV and 30 keV. We used Ag density: 10.5 g/cm^3, Ag bulk plasmon energy 3.78 eV, and Ag work function 4.64 eV.

5) Analytical SE model

The analytical model for $I_{cube}(x)$ in Eq. (1) has three factors:

a) $C_{SE}(x',x)$

The SE generation density $C_{SE}(x',x)$ as a function of position x' for an electron incident at x in a vertical plane centered in the Ag nanocube, integrated over the nanocube height, is modeled using a Gaussian distribution:

$$C_{\mathrm{SE}}(x',x) = \begin{cases} \frac{N_{\mathrm{SE}}}{\sigma_{\mathrm{g}}\sqrt{2\pi}} exp\left(-\frac{(x'-x)^2}{2\sigma_{\mathrm{SE}}^2}\right) & \frac{-D}{2} < x' < \frac{D}{2} \text{ and } \frac{-D}{2} < x' < \frac{D}{2} \\ 0 & \text{elsewhere} \end{cases} \quad \text{(S1)}$$

with N_{SE} the number of secondary electrons generated per primary electron, σ_{SE} the standard deviation, and D the nanocube size.

b) $P_{esc}(x')$

The probability $P_{esc}(x')$ that a SE generated at a position x' escapes from the nanocube (integrated over the nanocube height) so it can be detected is modeled using:

$$P_{\mathrm{esc}}(x') = P_{\mathrm{side}}(x') + P_{\mathrm{top}} \qquad \text{(S2)}$$

with P_{top} the probability for SEs escaping from the top, which we assume to be independent of x', and $P_{side}(x')$ the probability for SEs to escape from the side facets which is modeled using:

$$P_{\mathrm{side}}(x', \sigma_{\mathrm{esc}}, D) = \int_{-\frac{D}{2}}^{\infty} P_{\mathrm{s}} \exp\left(-\frac{(x'+\frac{D}{2})^2}{2\sigma_{\mathrm{esc}}^2}\right) + \int_{-\infty}^{\frac{D}{2}} P_{\mathrm{s}} \exp\left(-\frac{(x'-\frac{D}{2})^2}{2\sigma_{\mathrm{esc}}^2}\right) \qquad \text{(S3)}$$

with σ_{esc} the effective electron escape depth from the cube and P_S a scaling factor.

c) $B(x,\sigma_{beam})$

The integral over $C_{SE}(x',x)P_{esc}(x')$ in Eq. (1) is convolved with the beam profile that is modeled using a Gaussian distribution:

$$B(x, \sigma_{\mathrm{beam}}) = \frac{1}{\sigma_{\mathrm{beam}}\sqrt{2\pi}} \exp\left(-\frac{x^2}{2\sigma_{\mathrm{beam}}^2}\right) \qquad \text{(S4)}$$

with σ_{beam} the standard deviation. We use effective beam widths of 2 nm and 12 nm FWHM, corresponding to σ_{beam} = 0.85 nm and σ_{beam} = 5.1 nm.

The simulated SE coefficient as a function of beam position in Figures 2b,d was then fitted with Eqn. (1), using as free parameters the width of the SE distribution σ_{SE}, the escape depth σ_{esc} and the product $N_{SE}P_S$. The resulting function $N_{SE}P_{esc}(x')$ is plotted in Figures 2a,c for the two beam widths and beam energies. At each energy and beam width similar graphs $P_{esc}(x')$ for values for P_{top} and P_S are found for the fits for the two different beam widths (σ_b), as expected.

As described in the main text the analytical model for $I_{cube}(x)$ in Eq. (1) was also used to fit the SE line profiles with the beam width as a free parameter. A beam width of σ_{beam}=5-6 nm was consistently found for the best beam alignment conditions.

6) MNPBEM simulations

MNPBEM calculations were made for Ag nanocubes in vacuum using a cubic mesh with a size of 3.5 nm. Particles were marginally rounded (default value). Optical constants for Ag were taken from Ref. 3 and the beam width was 0.2 nm. Using the retarded MNPBEM beam solver the angle-dependent radiation patterns were derived from the calculated surface charges and currents. The CL spectrum was then obtained by collecting all emission over all angles.

7) Analytical CL model

The CL signal across the nanocube is modeled using the following qualitative model:

$$I_{\mathrm{CL}}(x, L, a, b, D) = \begin{cases} (a+b)\exp\left(\frac{x+\frac{D}{2}}{L}\right) & x < -\frac{D}{2} \\ a + b\left[\exp\left(-\frac{x-\frac{D}{2}}{L}\right) + \exp\left(\frac{x+\frac{D}{2}}{L}\right)\right] & -\frac{D}{2} < x < \frac{D}{2} \\ (a+b)\exp\left(-\frac{x-\frac{D}{2}}{L}\right) & x > \frac{D}{2} \end{cases} \qquad \text{(S5)}$$

This equation reflects the CL plateau observed the particle top with amplitude a, the exponential decay outside the cube ($x<-D/2$ and $x>D/2$) with amplitude ($a+b$) at the particle edge and characteristic decay length L, and the two exponential tails on top of the particle, with amplitude b and the same characteristic decay length L. Similar to the case for $I_{cube}(x)$ above we convolute $I_{CL}(x)$ with the Gaussian distribution Eq. S4 that reflects the effective beam width. The beam widths found from the fit of the CL profiles are σ_b=5-6 nm for the best beam alignment conditions, and are linearly correlated with the beam widths derived from the fits of the SE data.

References

1. Brenny, B. J. M., Coenen, T. & Polman, A. Quantifying coherent and incoherent cathodoluminescence in semiconductors and metals. *J. Appl. Phys.* **115,** 244307 (2014).
2. Tao, A., Sinsermsuksakul, P. & Yang, P. Polyhedral silver nanocrystals with distinct scattering signatures. *Angew. Chemie - Int. Ed.* **45,** 4597–4601 (2006).
3. Johnson, P.B., and Christy, R. W. Optical constants of the noble metals. *Phys. Rev. B* **6,** 4370 (1972).